ABSTRACT

Rutherford developed his revolutionary model of the atom based on experiments using helium nuclei scattered by a thin gold foil. In this paper, we review the measurements of the size of the helium nucleus, focusing on spectroscopic techniques. We touch on the "proton radius puzzle" that has incited a great deal of interest in high resolution spectroscopy of the most fundamental atoms. We find that for an absolute value of the size of the helium nucleus, the theoretical advance that will give a new determination is just around the corner.

KEYWORDS

Laser spectroscopy, Atomic Physics, Atomic structure, Quantum Electrodynamics

REVIEW ARTICLE

The size of the helium nucleus: Then and Now

M.D. Hoogerland

Dodd-Walls Centre for Photonic and Quantum Technologies, Department of Physics, University of Auckland, Private Bag 92019, Auckland, New Zealand

ARTICLE HISTORY
Compiled July 23, 2021

1. Introduction

At the start of the 20th century, the prevailing model for the atom was the Thomson "plum pudding" model. In this model, the charges are distributed over the size of the atom, which was known to be in the order of Ångstroms (10^{-10} m). To investigate whether this model was correct, and in collaboration with Rutherford, Hans Geiger and Ernest Marsden performed an experiment, in which they scattered highly energetic α-particles (now known to be nuclei of the helium atom) off a gold foil. It was found that the α-particles could be deflected over a large range of angles, including some that were scattered back towards the source. On the other hand, most α-particles went through without being deflected at all.

Both of these observations were at odds with the plum pudding model of the atom. In particular, if the charges and mass are roughly evenly distributed across the atom, most particles should show some deflection, as there would be no way to get through without interaction. On the other hand, an interaction with a distributed charge would result in a small deflection, as the α-particles had quite a high energy ($\sim$5 MeV). From this, Rutherford deduced that most of the mass and the positive charge of the atom must be concentrated in a small nucleus, thereby negating the "plum pudding" model of the atom with a distributed charge. In contrast, if the mass and positive charge were concentrated in the nucleus, α-particles missing this nucleus would zip right through, and α-particles hitting the nucleus would be able to be scattered under large angles. From this conclusion, the immediate question arises:

How big is this nucleus?

In his paper, Rutherford (1911) was able to derive that the charge on the gold nucleus would have to be about 100 electron charges (we now know it is 79 electron charges). It turned out much later, that the radius of a gold nucleus is $\sim$7.0 fm. This is to be compared to the radius of the electron cloud, which is about 150,000 fm. The atom is indeed quite empty! Furthermore, Rutherford and Royds (1908) showed that α particles were actually ionised helium nuclei. In this review, we will explore the size of the α-particle, as it has been found then and now.

2. Electron scattering

The currently accepted value for the radius of the alpha particle from a range of electron scattering experiments is 1.681±0.004 fm Sick (2008). The principle of the experiment has not changed since the first measurement from high-energy electron scattering, published by McAllister and Hofstadter (1956). The accuracy has however evolved considerably. The most accurate experiment to date has been published by Ottermann et al. (1985), by now already some time ago. They used a pressurised gas container in an evacuated detection chamber, and performed an angle-resolved scattering experiment using a 188 MeV incident electron beam. The differential cross-section was measured, and it was found that the best agreement was for a charge radius of 1.60±0.10 fm. In figure 1, we show the basic principle of the differential cross-section experiment carried out in this paper.

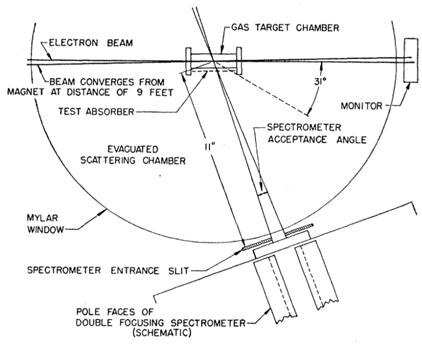

Figure 1. The electron scattering experiment, in which the angular deflection of electrons scattered from the gas target chamber is measured by the double focusing electron spectrometer. From reference McAllister and Hofstadter (1956)

3. Spectroscopic measurements

Over the past century, the framework of quantum mechanics has been found to be very powerful. Solving the spatial Schrödinger equation, one is able to find the rough structure of the Hydrogen atom, and solve for the shape of the electron wave function. Then, the addition of spin to the electron and the nucleus add a number of features, giving quite a good prediction of the level structure. Finally, Quantum-Electro-Dynamics (QED) corrections yield an extremely accurate picture of the energy levels.

With recent advances in spectroscopy, it is now possible to “count” optical cycles of a spectroscopy laser beam, as reviewed in Picqu and Hnsch (2019). In short, a beat signal is generated with a mode-locked laser, which has a frequency spectrum with a large number of equally spaced peaks at frequencies

$$f_n = f_0 + n f_r \ , \tag{1}$$

a “frequency comb”. One of these frequencies f_n is near enough to the spectroscopy laser frequency so that the beat frequency is in the radio-frequency (RF) region, and can be measured with a standard RF counter. The number n can be determined with a standard wavelength meter on the spectroscopy laser. The repetition frequency f_r is

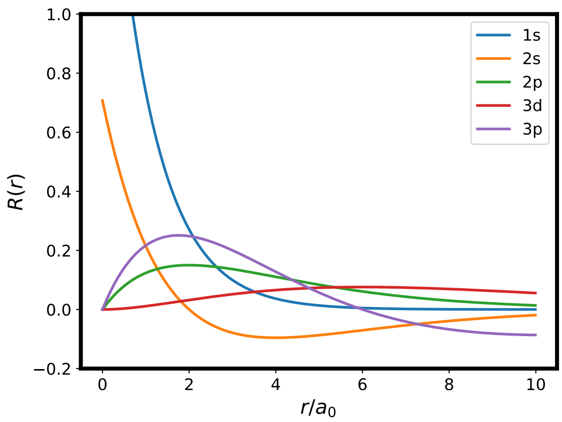

Figure 2. The radial wave functions in hydrogen. There is a significant fraction of the wave function inside the nucleus at $r = 0$, particularly for $l = 0$ states (1s and 2s in the figure). The horizontal axis is scaled by the Bohr radius a_0.

also in the RF, and can easily be measured. Finally f_0, which is less than f_r, can be determined by frequency doubling the frequency comb, and beating a low frequency component of this doubled beam to a high frequency component of the original laser beam. The beat frequency is f_0, which can then be measured and locked.

3.1. Background

The radial part of the Schrödinger equation for an electron in a central potential with charge Z reads

$$-\frac{\hbar^2}{2m}\frac{d^2u}{dr^2} + \left[-\frac{Ze^2}{4\pi\epsilon_0 r} + \frac{\hbar^2}{2m}\frac{l(l+1)}{r^2}\right]u = Eu \tag{2}$$

with radial wave functions as illustrated in Figure 2. From these distributions, it is apparent that there is a finite probability for the (2s) electron to be inside the nucleus. Here, the Bohr radius $a_0 = 4\pi\epsilon_0\hbar^2/(m_e e^2)$, with ϵ_0 the permittivity of the vacuum, the reduced Planck's constant $\hbar$, the electron mass m_e and the electron charge e.

A correction for the size of the nucleus can be found by considering the nucleus as a charged conducting sphere with radius R_n, and we set the potential to being constant inside this sphere. The correction can then be found by standard first order perturbation theory. It should be noted that for normal atoms the radius of the nucleus R_n is four orders of magnitude smaller than the Bohr radius a_0, and that hence the energy shift is small.

The radial wave functions plotted in figure 2 are for Hydrogen, and are exact solutions. The available wave functions for helium are approximations, but Drake and Yan (1992) worked these out to an acceptable precision by to calculate the correction to the energy levels due to the electron wave function being inside the nucleus. Using these, Morton et al. (2006) determined the helium spectrum to a high level of accuracy, but without the influence of the size of the nucleus. Quantum Electro-Dynamics (QED) corrections, as calculated in this paper, are worked out in powers of the fine structure constant. By measuring the spectrum of helium with high resolution, and finding the difference with the theoretical prediction, a value for the charge radius of the nucleus can be found.

An interesting twist is that the QED corrections are identical for ^{4}He and its isotope ^{3}He. Hence the uncertainties introduced by these imperfect corrections are cancelled when the isotope shift is used to find the difference in radius between these two nuclei. As the radius of the alpha particle is relatively well known, this could then serve as a measurement of the ^{3}He nucleus. This charge radius is actually larger than that of the alpha particle, even though it has fewer nucleons.

3.2. Proton radius puzzle

As the structure of the hydrogen atom can be calculated exactly, excluding the charge radius of the nucleus (a proton), hydrogen was a prime candidate for a spectroscopic experiment, where the energy difference between two states is measured with great accuracy. A number of spectroscopic measurements before 2010 agreed with the results from electron scattering as given by the CODATA value as can be found in Mohr et al. (2016).

However, in 2010, everything changed with an experiment using muonic hydrogen Pohl et al. (2010). In this experiment, the electron is replaced by a muon. As muons and electrons, according to the standard model, differ only by their masses, this should be a straightforward replacement. The advantage of using muons, which have a mass about 200 times larger than the electron, is that, as the Bohr radius a_0 scales inversely with the mass of the "electron", the larger mass of the muon gives a 200 times smaller radius of its orbit. Hence the size of the nucleus would yield a few million times larger correction to the energy levels.

The main difficulty with these experiments is of course that one needs muons to begin with, and these are produced in a nuclear reactor. In a landmark experiment, Pohl et al. (2010) found a value for the charge radius of the proton of $r_p = 0.84184(67)$ fm, which was as much as 5σ smaller than the accepted value of 0.8768(69) fm.

This lead to a great deal of excitement, as any differences between hydrogen and muonic hydrogen could point to physics beyond the standard model. For a treatise on the standard model, refer to Oerter (2006). The precision of the muonic hydrogen result is also helped by significant theoretical insight in its level structure, as worked out by Antognini et al. (2013) and by Indelicato (2013).

An interesting development came in 2017, when new results in normal hydrogen by Beyer et al. (2017) agreed with the muonic measurements and put the radius of the proton at $r_p = 0.8335(95)$ fm. This was recently corroborated by a new result on the 2s–2p splitting by Bezginov et al. (2019), which claims $r_p = 0.833(10)$ fm.

A recent review by Karr and et E. Voutier. (2020) beautifully summarises the efforts to date to find the charge radius of the proton as well as that of the alpha particle. They expect that the discrepancy between the CODATA value and the new spectroscopic results will be resolved by better accuracy in both the scattering and spectroscopic experiments contributing to this CODATA value, and that the muonic hydrogen result will confirmed by more normal hydrogen experiments in the future.

Very recently however, an experiment by Abi et al. (2021) shows a deviation of 4.2σ of the muon magnetic moment from its theory prediction. This indicates that lepton universality, meaning that a muon should behave identically to an electron apart from the mass, is violated. Will this mean that there is new physics in the muonic atom experiments, and the proton radius is closer to the CODATA value after all?

It is this author's view that this issue is far from resolved, as many measurements contribute to the CODATA value for the charge radius of the proton. We may see more evidence of physics beyond the standard model emerging from high accuracy experiments, and the proton radius puzzle may have only been the first of the road signs along the way.

4. Helium Experiments

A good candidate for the determination of the charge radius of the helium nucleus is afforded by the $2^3S \rightarrow 2^3P$ transition frequencies, which are around 1083 nm. As can be seen in Fig. 2, the $2s$ metastable lower state overlaps with the nucleus, whereas the $2p$ excited state has a significantly reduced overlap, as the amplitude of the wave function at $r = 0$ is zero for a p-state. However, these transitions are dipole allowed, and hence have a line width of $\sim$1.6 MHz, much larger than the shift induced by the finite size of the nucleus. In an atomic beam experiment, careful spectroscopy by Pastor et al. (2004) of this transition has allowed for a new determination of the Lamb shift of the 2^3P states in helium.

A narrow transition in helium, which would allow for a more precise measurement of the transition frequency, is found in the 2^3S$\rightarrow$ 2^1S transition, which is dipole and spin forbidden. The linewidth of this transition is $\Gamma = 2\pi \cdot 8$ Hz and the transition wavelength is around 1557 nm, in the telecom bracket. This line width is due to spontaneous decay of the 2^1S state to the ground 1^1S state, but due to the twice forbidden nature of the transition, the 2^3S$\rightarrow$ 2^1S transition has an Einstein A coefficient of $A \approx 9 \cdot 10^{-8}$s^{-1}, which should be compared to $A \approx 10^7$ s^{-1} for the allowed transition discussed above. To excite the forbidden transition, a narrow-band laser is required as well as a long interaction time.

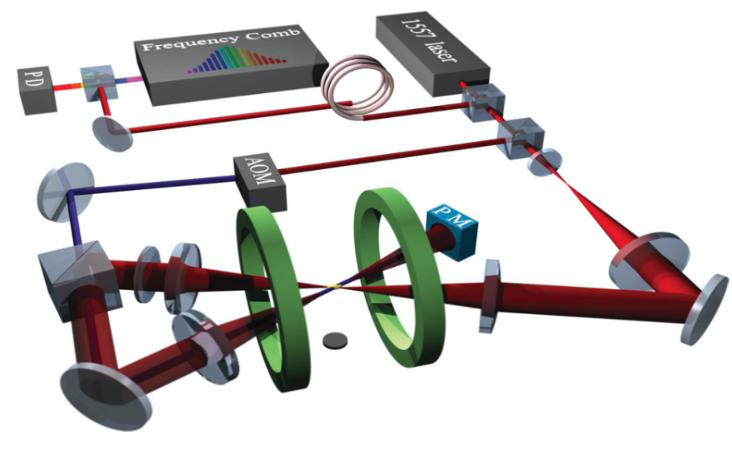

Figure 3. Schematic representation of the experiment by Van Rooij et al. (2011)

The first experiment exciting this transition and performing a high-resolution spectroscopy experiment on both isotopes of helium was published by Van Rooij et al. (2011), who used the setup illustrated in Fig **??**. A Bose-Einstein Condensate of metastable 2^3S atoms was captured in a dipole trap, formed by a laser close to resonance with the forbidden transition. The ultracold atom sample and conservative dipole trap allowed interaction times of up to six seconds. For the fermionic ^{3}He isotope, a degenerate Fermi gas was captured in the same trap. It should be noted that the hyperfine interaction adds an additional frequency shift, but that is known very accurately. The precision of this experiment for both isotopes was one part in 10^{11}, limited by the laser linewidth and the large AC Stark shift of the atoms in the trap. The radius of the ^{3}He nucleus was determined to be 1.961(4) fm at the time. This was also limited by the accuracy of the QED corrections applied, which went up to α^4. As mentioned, the QED corrections cancel when the difference in radius is investigated, and the difference in radii squared $\Delta r_c^2 = r_c^2(^3\mathrm{He}) - r_c^2(^4\mathrm{He})$ is proportional to the isotope shift. In this experiment, the difference Δr_c^2 =1.019(11) fm^2 . This agreed reasonably well with a previous determination using the 2^3S→ 2^3P$_0$ transition, which yielded $\Delta r_c^2 = 1.059(3)$ fm^2.

A little later, experiments by Cancio Pastor et al. (2012), using spectroscopy on the 2^3S→ 2^3P transitions, have also determined the difference between the charge radii of ^{4}He and ^{3}He, and found a significant shift of the transition frequency due to the size of the nucleus. More recent experiments on this same transition in ^{4}He by Zheng et al. (2017), using the ^{3}He data from Cancio Pastor et al. (2012), put the difference in charge radii to $\Delta r_c^2 = 1.028(2)$ fm^2, in good agreement with the ultracold atom experiment by Van Rooij et al. (2011), but with a higher precision.

A second generation of the ultracold atom experiment used a more narrow-band laser (linewidth 500 Hz) and a special magic wavelength trap, where the AC Stark shifts of the ^{3}S and ^{1}S states are identical. The 319 nm laser trap, described by Rengelink et al. (2016), was necessarily within a nanometre to an allowed transition, which led to a significant spontaneous emission rate. Therefore, interaction times where limited to one second. However, the reduced laser linewidth more than made up for the reduced interaction time, and the transition frequency could be determined to 1 part in 10^{12} for ^{4}He, a factor of 10 improvement, as reported by Rengelink et al. (2018). The experiment on ^{3}He is currently under way. Given the previous determination of the ^{3}He transition frequency, combined with the new determination of the ^{4}He frequency, yielded a difference in charge radius of the nuclei of $\Delta r_c^2 = 1.041(7)$fm^2. If the new determination of the ^{3}He isotope yields a similar precision as the ^{4}He measurement, the precision of the difference in radii will reduce to less than 0.002 fm^2.

In the singlet part of the spectrum, a new spectroscopic measurement by Huang et al. (2020) on the 2^1S→3^1D$_2$ two-photon transition have also come to a determination of the difference in charge radius. This experiment uses a fluorescence method in a gas cell. The wavelength of the two-photon transition is 1009 nm. They determine the isotope shift to be 29.530246(18) GHz, leading to a derived difference in charge radius of $\delta r_c^2 = 1.059(25)$ fm^2.

Another experimental effort focuses on spectroscopy of the helium ion He$^+$. As the helium ion only has one electron, like hydrogen, the level structure is exact. Again, the focus is on the two photon 1s–2s transition. In a new experimental effort, He$^+$ ions are trapped and sympathetically cooled by beryllium ions. This eliminates the Doppler shift and increases the interaction time. The interrogation is then carried out with a 30 nm photon, generated by high-harmonic generation, and a 790 nm photon, as detailed in Krauth et al. (2019).

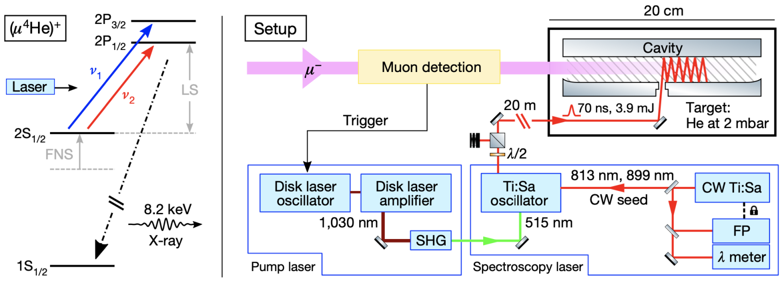

Figure 4. Schematic representation of the experiment by Krauth et al. (2021)

5. Exotic helium experiments

Very recently, the first result has been published on the charge radius of the helium nucleus using muonic helium by Krauth et al. (2021). This exciting new development benefits from the same increased sensitivity and a more convenient wavelength as the muonic hydrogen measurement discussed earlier. In fact the finite size of the nucleus accounts for 20% of the splitting between the 2s and 2p states. The linewidth of the observed 2s–2p transitions observed (319 GHz) is much larger than those used in normal atoms, leading to a 15 GHz precision on the frequency of the line centre, but that is more than offset by the gains in sensitivity. Their measurement of the radius of the α-particle $r_\alpha = 1.67824(13)_{\mathrm{exp}}(82)_{\mathrm{theo}}$ fm is the most accurate to date. As illustrated in Fig. 3, slow muons are decelerated by collisions with helium gas atoms. In the last collision, the muon takes the place of one of the electrons. The second electron is rapidly ejected by the internal Auger process, yielding a single muon bound to a helium nucleus, typically in a highly excited state. About 1% of the atoms decays into the 2s metastable state. A pulsed laser is triggered when a muon enters the detection chamber and performs an excitation to the 2p state, and the decay to the 1s ground state is observed through the emission of an X-ray photon subsequent to the laser pulse.

As with hydrogen, the muonic determination of the nuclear radius is by far more precise than previous spectroscopic determinations. It does however depend on lepton universality, which may be violated by physics beyond the standard model. This is an exciting development, and new spectroscopic determinations in normal helium are essential to understand this new physics.

A further recent development is the laser spectroscopy of pionic helium, as reported by Hori et al. (2020). A negatively charged pion π^-, formed by a down quark and an up antiquark, can also replace the electron in a helium atom. The pion is absorbed by the nucleus quickly, but there are some highly excited metastable states with lifetimes in the nanosecond region. As these highly excited states are relatively far removed from the nucleus, little information on the size of the nucleus can be expected from pion spectroscopy, but it may lead to insight into physics beyond the standard model.

6. Helium theory

Work is also continuing on the theoretical determination of the relativistic corrections to the helium spectrum. A recent advance by Patkóš et al. (2020) has now worked out the corrections to the triplet states in helium to 7th order in the fine structure constant. However, the numerical value of the correction, which would allow, in combination with the experimental results, for an absolute determination of the charge radius of the α-particle, has not been completed yet. This numerical value should not take long to find, and we look forward to an exact determination.

A significant body of work working out the theory of the Lamb shift and fine structure in muonic helium has been published by Diepold et al. (2018) and also for ^{3}He by Franke et al. (2017). The accuracy achieved in the muonic helium experiments is clearly helped by these detailed investigations.

7. Conclusion

The size of the alpha particle, or rather its charge radius, remains an interesting testbed for QED and Quantum Chromo Dynamics (QCD) calculations. Since the days of Rutherford there have been extensive experiments on the charge radius of the helium nucleus using electron scattering, yielding a value accurate to a few parts per thousand. The latest spectroscopic determination using muonic helium yielded a result for the charge radius with a precision of a few parts per million. The spectroscopic measurement of the transition frequencies in normal helium are accurate to one part in 10^{12}, and combined with state-of-the-art calculations of the QED corrections to the level structure, should also yield an accurate determination of the helium nuclear charge radius. It will be interesting to see how that compares to the muonic helium measurement. More than a century after Rutherford's revolutionary model of the atom, there is still plenty to discover in the structure of the atom.

Acknowledgement

The author would like to thank S. Shamailov for carefully reading the manuscript.

References

Abi B, Albahri T, Al-Kilani S, Allspach D, Alonzi LP, Anastasi A, Anisenkov A, Azfar F, Badgley K, Baeßler S, et al. (Muon $g-2$ Collaboration). 2021. Measurement of the positive muon anomalous magnetic moment to 0.46 ppm. Phys Rev Lett. 126:141801. Available from: https://link.aps.org/doi/10.1103/PhysRevLett.126.141801.

Antognini A, Kottmann F, Biraben F, Indelicato P, Nez F, Pohl R. 2013. Theory of the 2s2p lamb shift and 2s hyperfine splitting in muonic hydrogen. Annals of Physics. 331:127–145.

Beyer A, Maisenbacher1 L, Matveev A, Pohl R, Khabarova K, Grinin1 A, Lamour T, Yost DC, Hänsch TW, Kolachevsky N, et al. 2017. The rydberg constant and proton size from atomic hydrogen. Science. 358:79–85.

Bezginov N, Valdez T, Horbatsch M, Marsman A, Vutha AC, Hessels EA. 2019. A measurement of the atomic hydrogen lamb shift and the proton charge radius. Science. 365:10071012.

Cancio Pastor P, Consolino L, Giusfredi G, De Natale P, Inguscio M, Yerokhin VA, Pachucki K. 2012. Frequency metrology of helium around 1083 nm and determination of the nuclear charge radius. Phys Rev Lett. 108:143001. Available from: https://link.aps.org/doi/10.1103/PhysRevLett.108.143001.

Diepold M, Franke B, Krauth J, Antognini A, Kottmann F, Pohl R. 2018. Theory of the lamb shift and fine structure in muonic 4he ions and the muonic 3he–4he isotope shift. Annals of Physics. 396:220–244.

Drake G, Yan ZC. 1992. Energies and relativistic corrections for the rydberg states of helium: Variational results and asymptotic analysis. Phys Rev A. 46:2378.

Franke B, Krauth J, Antognini A, Diepold M, Kottmann F, Pohl R. 2017. Theory of the n=2 levels in muonic helium-3 ions. Eur Phys J D. 71:341.

Hori M, Aghai-Khozani, H S, et al A. 2020. Laser spectroscopy of pionic helium atoms. Nature. 581:3741.

Huang YJ, Guan YC, Peng JL, Shy JT, Wang LB. 2020. Precision laser spectroscopy of the $2^1s_0 - -3^1d_2$ two-photon transition in ^{3}He. Phys Rev A. 101:062507. Available from: https://link.aps.org/doi/10.1103/PhysRevA.101.062507.

Indelicato P. 2013. Nonperturbative evaluation of some qed contributions to the muonic hydrogen n=2 lamb shift and hyperfine structure. Phys Rev A. 87:022501.

Karr JP, et E Voutier DM. 2020. The proton size. Nature Reviews Physics. 2:601–614.

Krauth J, Dreissen L, Roth C, Grndeman E, Collombon M, Favier M, Eikema K. 2019. Paving the way for fundamental physics tests with singly-ionized helium. PoS FFK2019. 049.

Krauth J, Schuhmann K, Ahmed M, Amaro F, Amaro P, Biraben F, Chen TL, Covita D, Dax A, Diepold M, et al. 2021. Measuring the α-particle charge radius with muonic helium-4 ions. Nature. 589:527–531.

McAllister RW, Hofstadter R. 1956. Elastic scattering of 188-mev electrons from the proton and the alpha particle. Phys Rev. 102:851–856. Available from: https://link.aps.org/doi/10.1103/PhysRev.102.851.

Mohr PJ, Newell DB, Taylor BN. 2016. Codata recommended values of the fundamental physical constants: 2014. Rev Mod Phys. 88:035009. Available from: https://link.aps.org/doi/10.1103/RevModPhys.88.035009.

Morton DC, Wu Q, Drake GWF. 2006. Energy levels for the stable isotopes of atomic helium (4he i and 3he i). Can J Phys. 84:83–105.

Oerter R. 2006. The theory of almost everything: The standard model, the unsung triumph of modern physics (kindle ed.). Penguin Group.

Ottermann C, Kbschall G, Maurer K, Rhrich K, Schmitt C, Walther V. 1985. Elastic electron scattering from 3he and 4he. Nuclear Physics A. 436(4):688 – 698. Available from: http://www.sciencedirect.com/science/article/pii/0375947485905548.

Pastor PC, Giusfredi G, Natale PD, Hagel G, de Mauro C, Inguscio M. 2004. Absolute frequency measurements of the $2^3S_1 \rightarrow 2^3P_{0,1,2}$ atomic helium transitions around 1083 nm. Phys Rev Lett. 92:023001. Available from: https://link.aps.org/doi/10.1103/PhysRevLett.92.023001.

Patkóš Vcv, Yerokhin VA, Pachucki K. 2020. Nonradiative α^7m qed effects in the lamb shift of helium triplet states. Phys Rev A. 101:062516. Available from: https://link.aps.org/doi/10.1103/PhysRevA.101.062516.

Picqu N, Hnsch T. 2019. Frequency comb spectroscopy. Nature Photon. 13:146157. Available from: https://doi.org/10.1038/s41566-018-0347-5.

Pohl R, Antognini A, Nez F, et al. 2010. The size of the proton. Nature. 466:213216.

Rengelink RJ, Notermans RPMJW, Vassen W. 2016. A simple 2w continuous-wave laser system for trapping ultracold metastable helium atoms at the 319.8 nm magic wavelength. Appl Phys B. 122:122.

Rengelink RJ, van der Werf Y, Notermans RPMJW, Jannin R, Eikema KSE, Hoogerland MD, Vassen W. 2018. Precision spectroscopy of helium in a magic wavelength optical dipole trap. Nature Physics. 107(11):1–1137.

Rutherford E. 1911. The scattering of α and β particles by matter and the structure of the atom. Philosophical Magazine, Series 6. 21:669–688.

Rutherford E, Royds T. 1908. Spectrum of the radium emanation. Philosophical Magazine, Series 6. 16:313317.

Sick I. 2008. Precise root-mean-square radius of ^{4}He. Phys Rev C. 77:041302. Available from: https://link.aps.org/doi/10.1103/PhysRevC.77.041302.

Van Rooij R, Borbely JS, Simonet J, Hoogerland MD, Eikema KSE, Rozendaal RA, Vassen W. 2011. Frequency Metrology in Quantum Degenerate Helium: Direct Measurement of the 2

$^3S_1 \rightarrow 2\ ^1S_0$ Transition. Science. 333(6039):196–198.

Zheng X, Sun Y, Chen J, Jiang W, Pachucki K, Hu S. 2017. Measurement of the frequency of the $2\ ^3s - 2\ ^3p$ transition of ^{4}He. Phys Rev Lett. 119:263002.